

Low-temperature anomalies in magnetic, transport, and thermal properties of single-crystal CeRhSn with valence fluctuations

M. S. Kim, Y. Echizen, K. Umeo, S. Kobayashi, M. Sera, P. S. Salamakha, O. L. Sologub, and T. Takabatake
Department of Quantum Matter, ADSM, Hiroshima University, Higashi-Hiroshima, 739-8530, Japan

X. Chen
Department of Applied Chemistry, Graduate School of Engineering, Hiroshima University, Higashi-Hiroshima, 739-8527, Japan

T. Tayama and T. Sakakibara
Institute for Solid State Physics, University of Tokyo, Kashiwa, 277-8581, Japan

M. H. Jung*
NHMFL, Los Alamos National Laboratory, Los Alamos, New Mexico 87545, USA

M. B. Maple
Department of Physics and Institute for Pure and Applied Physical Sciences, University of California, San Diego, La Jolla, California 92093-0360, USA

(Received 2 January 2003; revised manuscript received 22 April 2003; published 20 August 2003)

Magnetic, transport, thermal, and crystallographic properties are reported for single crystals of CeRhSn crystallizing in the hexagonal ZrNiAl-type structure. We found high anisotropy in both electrical resistivity ($\rho_a \approx 5\rho_c$ at 70 K) and magnetic susceptibility ($\chi_c \approx 10\chi_a$ at 0.4 K), which is atypical for a valence-fluctuating Ce compound. At low temperatures, $\rho(T)$ and $\chi(T)$ show power-law behaviors; $\rho_a(T) \propto T^{1.5}$ and $\rho_c(T) \propto T$, and $\chi_a \propto T^{-0.35}$ and $\chi_c \propto T^{-1.1}$ down to 0.4 K. These behaviors and the rather large residual resistivity were not affected by long-term annealing. On cooling from 7 K to 0.5 K, the specific heat divided by temperature C/T increased as $-\ln T$ and saturated to a rather large value of 0.2 J/mol K². These experimental results are discussed in relation to the possible atomic disorder.

DOI: 10.1103/PhysRevB.68.054416

PACS number(s): 75.20.Hr, 72.15.Qm, 75.30.Mb

I. INTRODUCTION

Cerium-based equiatomic compounds CeTX, where T is a transition metal and X is a p -electron element, have received much attention in recent years because they exhibit anomalous physical properties such as heavy-fermion behavior, valence fluctuations, and hybridization gap behavior.¹ Most of CeTX systems with $T = \text{Rh}$ exhibit valence fluctuations for various X elements Al, P, As, In, and Sb,²⁻⁶ suggesting strong hybridization of the Ce $4f$ state with the Rh $4d$ band. CeRhSn was also classified into the valence-fluctuating system, because the temperature dependence of the magnetic susceptibility is much weaker than the Curie-Weiss behavior expected for trivalent Ce ions⁷ and the unit-cell volume is significantly smaller than that expected for trivalent-ion compounds on the basis of lanthanide contraction.⁸⁻¹¹ Recently, more direct evidence for valence fluctuations has been given by x-ray photoelectron spectroscopy measurements by Ślebarski *et al.*¹² Thereby, the Ce valence in CeRhSn has been estimated to be 3.07 at room temperature.

CeRhSn crystallizes in the hexagonal ZrNiAl-type structure.¹¹ Layers composed of Ce and Rh atoms alternate along the c axis with layers composed of Rh and Sn atoms. For polycrystalline samples, unusual magnetic properties have been reported.¹² Both the specific heat and magnetic susceptibility of an arc-melted sample showed distinct jumps at 6.2 K, in which the magnitude decreased by annealing at 800 °C for eight days but still remained after the heat treat-

ment for four weeks. Since no impurity phase was detected by powder x-ray and neutron-diffraction analyses, the phase transition at 6.2 K was attributed to a magnetic transition of a sort of magnetic phase produced by atomic disorder. At temperatures below 4 K, the specific-heat-divided temperature C/T followed the logarithmic temperature dependence, $C/T \propto -\ln T$. Furthermore, the electrical resistivity and magnetic susceptibility showed power-law temperature dependencies, $\rho(T) \propto T^{0.75}$ and $\chi(T) \propto T^{-0.5}$. These non-Fermi-liquid behaviors were interpreted as the proximity of the ground state of this compound to a quantum critical point.¹² The proximity seems to originate from the Griffiths singularities as a consequence of the interplay between an intrasite Kondo effect and intersite Ruderman-Kittel-Kasuya-Yosida interaction in the presence of disorder and magnetic anisotropy.¹³

For better understanding of the origin of the magnetic ordering and non-Fermi-liquid behavior in CeRhSn, it is important to study the magnetic and transport properties of single-crystalline samples because highly anisotropic behaviors are expected from the hexagonal ZrNiAl-type structure. For the isostructural compound CePdAl, e.g., the a -axis resistivity is approximately twice the c -axis resistivity over the temperature range 0.1–300 K,¹⁴ and the c -axis susceptibility is one order-of-magnitude larger than the a -axis susceptibility at the Néel temperature $T_N = 2.7$ K.¹⁵ Furthermore, the geometrical frustration of the Ce moments in the c -plane quasi-*kagomé* lattice allows one third of Ce ions to remain

paramagnetic even below T_N .¹⁶ Here, we report the thermal, transport, magnetic, and structural properties of single-crystal CeRhSn. Preliminary results have been reported in a conference paper.¹⁷

II. EXPERIMENT

Single crystals of CeRhSn and its reference compound LaRhSn were grown with the Czochralsky method from the melt of stoichiometric amounts of the constituent elements in an rf induction furnace. We obtained crystals that were 5 mm in diameter and 40 mm in length. From the top to the end of the crystal rod of CeRhSn, no deviation of the composition from the stoichiometric one was detected by electron-probe microanalysis. However, the presence of a spurious phase of CeRh₃ of less than 1% was detected at the end of the rod. To examine the effect of annealing on the physical properties, half of the crystal rod was wrapped with tantalum foils, sealed in an evacuated quartz tube, and annealed at 900 °C for three weeks.

The x-ray single-crystal data were collected using a Rigaku R-AXIS imaging plate area detector with graphite monochromated Mo $K\alpha$ radiation operating at 50 kV and 40 mA. A total of 55 oscillation images were collected using ω scans (width 5° and exposure time of 750 s per frame) and the raw intensity data were corrected for Lorentz and polarization effects, and for absorption by a Gaussian numerical integration using the measured dimensions of the crystal.

The electrical resistivity along the a and c axes was measured from 0.4 K to 300 K by a conventional four-probe method. The magnetic-field dependence of resistivity was measured up to 18 T for both transverse and longitudinal configurations. The Hall coefficient measurement was carried out by a dc technique in a field of 1 T on samples of 0.3 mm in thickness. The magnetic susceptibility for $2\text{ K} < T < 300\text{ K}$ was measured using a commercial superconducting quantum interference device magnetometer (MPMS, Quantum Design). The measurement of magnetization was performed down to 0.4 K with a Faraday force magnetometer at the Institute for Solid State Physics, University of Tokyo.¹⁸ The specific heat was measured by an adiabatic method and a relaxation method for $0.8\text{ K} < T < 70\text{ K}$ and $0.5\text{ K} < T < 5\text{ K}$, respectively.

III. RESULTS AND DISCUSSION

The crystal structure of CeRhSn was refined by a full-matrix least-squares program using atomic scattering factors provided by the program package SHELXL-97.¹⁹ The analysis confirmed that CeRhSn crystallizes in the ZrNiAl-type structure (space group $P\bar{6}2m$), and Ce, Rh1, Rh2, and Sn atoms occupy the $3f$, $1a$, $2d$, and $3g$ sites, respectively (see Fig. 1). To obtain the crystallographic parameters, it was assumed that there was no disorder between Rh and Sn atoms. The closeness of the atomic numbers for Rh and Sn prevented us from determining the possible atomic disorder between them. Atomic coordinates and thermal parameters are listed in Table I. The atomic positions are in good agreement with previous ones determined by neutron powder diffraction.¹² It

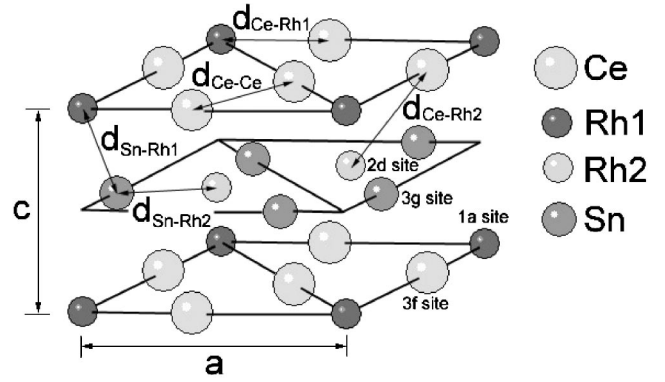


FIG. 1. Schematic representation of the unit cell of CeRhSn crystallizing in the hexagonal ZrNiAl-type structure. Lattice constants are $a=7.443(2)$ and $c=4.089(2)$, and interatomic distances are $d_{\text{Ce-Ce}}=3.8819(11)$, $d_{\text{Ce-Rh1}}=3.0838(10)$, $d_{\text{Ce-Rh2}}=3.0316(8)$, $d_{\text{Sn-Rh1}}=2.7622(9)$, and $d_{\text{Sn-Rh2}}=2.8424(9)$ Å.

should be noted that the displacement parameter $U_{33}=1.37 \times 10^{-2}$ Å² for Rh2 is twice or triple that of U_{11} for Rh2 and U_{33} for other atoms. Such an anisotropic displacement of the $2d$ site atom in the ZrNiAl-type structure was reported for YbPtSn.²⁰ It was interpreted as a result of the instability for the $2d$ site to split into two sites by forming a superstructure. However, our analysis of CeRhSn assuming a split position yielded no improvement of the reliability factor.

In order to consider the hybridization in CeRhSn from the viewpoint of the interatomic distances, we compare in Fig. 2 the lattice parameters for ZrNiAl-type rare-earth compounds RNiIn, RRhIn, and RRhSn, of which the Ce compounds show valence fluctuations.^{2,8-12} The hexagonal a parameters of the RRhSn series for $R=\text{La, Ce, Pr, and Nd}$ are significantly smaller than those of RNiIn and RRhIn. Since the atomic radii of In and Sn are almost the same, this feature suggests the occurrence of strong hybridization in the basal plane of Rh2 and Sn atoms. In the series of RNiIn and RRhIn compounds, the a parameter for $R=\text{Ce}$ deviates downward due to the valence fluctuations in the Ce compound. In the RRhSn series, however, the c parameter of CeRhSn contracts significantly. As a result of this contraction along the c axis, the distance between Ce and Rh2 ($d_{\text{Ce-Rh2}}=3.032$ Å) out of plane becomes smaller than $d_{\text{Ce-Rh1}}$ (3.084 Å) in the basal plane (see Fig. 1). Furthermore, four Rh2 atoms are located at that distance, whereas only one Rh1 atom is nearby. This may lead to strong hybridization of the Ce $4f$ state with the $4d$ band derived from the Rh2 atoms, and thus the valence-fluctuating state would be stabilized in CeRhSn. This conjecture is consistent with the band-structure calculation,¹² in which the $4d$ -electron density of states just above the Fermi level is larger for Rh2 atoms than for Rh1 atoms.

Figure 3(a) shows the temperature dependence of magnetic susceptibility χ on the as-grown single crystal for $B//a$ and $B//c$ in $B=0.1$ T. It is noteworthy that the annealed single crystal showed essentially the same results of $\chi(T)$ for $T > 2$ K. With decreasing temperature, χ_c increases steadily without showing any anomaly or maximum, while χ_a stays almost constant down to 50 K and then increase. The ratio

TABLE I. Crystallographic data for CeRhSn at 293 K [space group $P\bar{6}2m$ (No. 189), $Z=3$, $a=7.443(2)$ Å, $c=4.089(2)$ Å, $V=195.89$ Å³, $\rho=9.199$ g/cm³]. U_{eq} stands for the isotropic thermal parameter defined as one-third of the trace of the orthogonalized U_{ij} tensor. Number of reflections: 5166 measured, 648 unique, and 635 with $I_{obs}>2\sigma(I_{obs})$; 17 parameters refined; $\mu=32.47$ mm⁻¹, $2\Theta_{max}=90.05^\circ$, and range in hkl : ± 14 , ± 14 , and ± 8 ; residual values: $R1=0.0398$ and $wR2=0.0907$; goodness of fit=1.106 and $BASF=0.1732(2)$.

Atom	Site	Positional and displacement parameters U_{ij} (in 10^{-2} Å ²) for CeRhSn									
		x	y	z	U_{11}	U_{22}	U_{33}	U_{12}	U_{13}	U_{23}	U_{eq}
Ce	3f	0.58567(8)	0	0	0.434(17)	0.602(23)	0.598(19)	$1/2U_{22}$	0	0	0.526(14)
Rh1	1a	0	0	0	0.622(28)	U_{11}	0.469(36)	$1/2U_{11}$	0	0	0.571(20)
Rh2	2d	1/3	2/3	1/2	0.678(20)	U_{11}	1.371(36)	0.339(11)	0	0	0.909(18)
Sn	3g	0.24999(9)	0	1/2	0.465(23)	0.380(18)	0.619(22)	0.232(11)	0	0	0.479(14)

χ_c/χ_a increases to 10 at 2 K. The high anisotropy and the absence of a maximum are atypical for valence-fluctuating Ce compounds. However, the largely negative values of the paramagnetic Curie temperatures, $\theta_{//a}=-390$ K and $\theta_{//c}=-57$ K, are characteristic of a valence-fluctuation system. These values were obtained by fitting the data above 160 K with the formula $\chi(T)=\chi_0+C/(T-\theta)$. The fits yielded the effective magnetic moments of $1.85\mu_B$ and $1.23\mu_B$ for $B//a$ and $B//c$, respectively, which are much reduced from the $2.54\mu_B$ expected for a free Ce³⁺ ion. In order to detect the possible magnetic anomaly at about 6.2 K reported by Ślebarski *et al.*,^{12,21} we measured $\chi(T)$ of the as-grown crystal in a field of 5 mT after zero-field cooling and field cooling. As is shown in the inset, both sets of data are identical and exhibit no anomaly near 6.2 K, and thus no magnetic transition occurs in our single crystals even in the as-grown state.

In Fig. 3(b), the $\chi(T)$ data are plotted on a double loga-

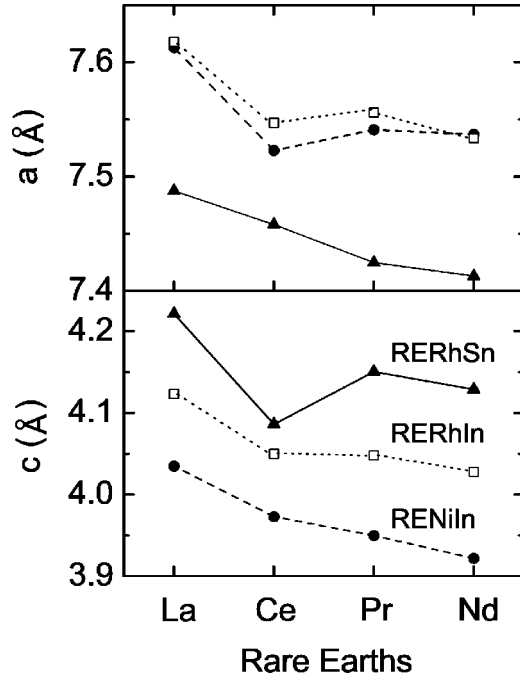


FIG. 2. Lattice constants a and c of the series RNiIn, RRhIn, and RERhSn ($R=La, Ce, Pr,$ and Nd) with the hexagonal ZrNiAl-type structure. The data for RNiIn are from Ref. 8; for RRhIn from Refs. 2, 9, and 10; and for RERhSn from Ref. 11.

arithmic scale. At temperatures below 2 K, the values of χ_c are depressed with increasing field from 0.05 T to 0.2 T, while χ_a is independent of the strength of B . The broken lines are the fits to the data of the equation $\chi(T)\propto T^{-n}$ with $n=0.35$ and 1.1 for $B//a$ and $B//c$, respectively. An intermediate value $n=0.5$ was reported for the $\chi(T)$ of a poly-

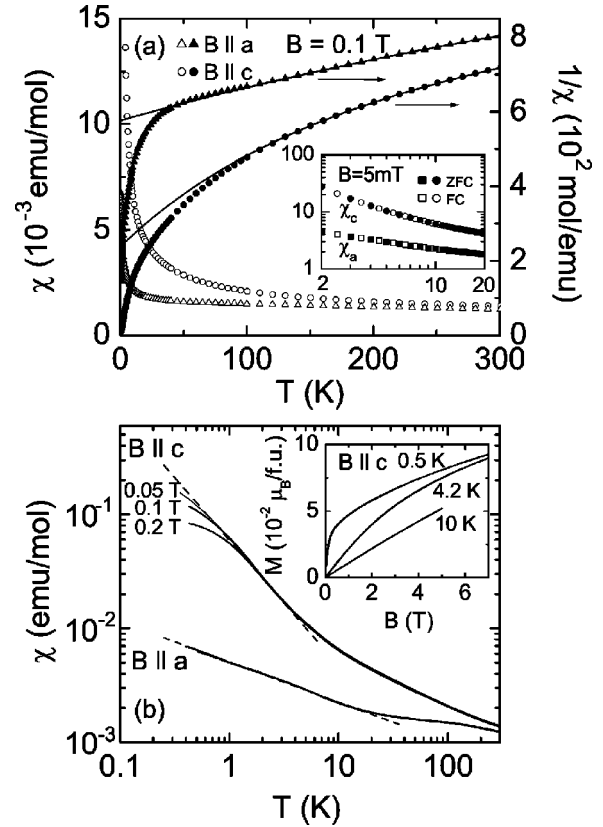


FIG. 3. (a) Temperature dependence of magnetic susceptibility χ and its inverse $1/\chi$ on as-grown crystal CeRhSn for $B//a$ and $B//c$ at $B=0.1$ T. The solid lines represent fits to the data of $\chi(T)=\chi_0+C/(T-\theta)$ for $160\text{ K}<T<300\text{ K}$. The inset of (a) shows a double logarithmic plot of χ vs T measured after zero-field cooling and field cooling in a field of 5 mT. (b) Double logarithmic plot of χ vs T at $0.4\text{ K}<T<300\text{ K}$ in $B=0.05, 0.1,$ and 0.2 T. The broken lines represent the power-law behavior $\chi(T)\propto T^{-n}$ with $n=0.35$ and 1.1 for $B//a$ and $B//c$, respectively. The magnetization curves $M(B//c)$ at 0.5, 4.2, and 10 K are displayed in the inset.

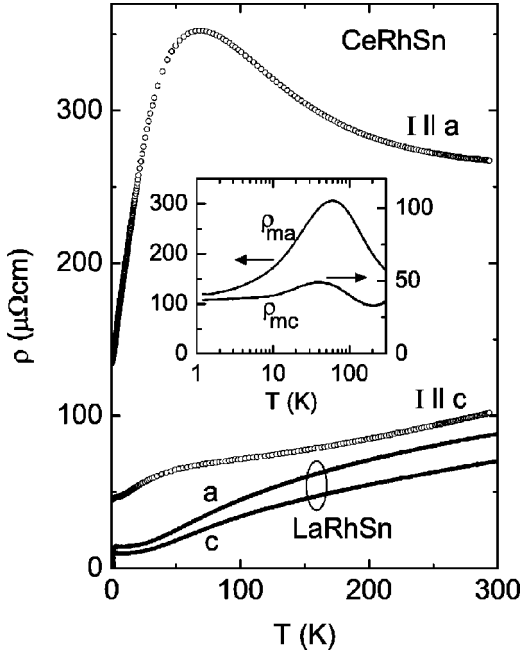


FIG. 4. Temperature dependence of the electrical resistivity for as-grown crystals of CeRhSn and LaRhSn along the *a* and *c* axes. The inset shows the magnetic contribution to the resistivity ρ_{ma} and ρ_{mc} on a logarithmic T scale.

crystalline sample in the temperature range from 2 to 30 K.¹² As a possible origin of the power-law behavior, non-Fermi-liquid nature due to atomic disorder was proposed,¹³ as mentioned in the Introduction. The Curie-like form observed for $\chi_c(T) = 0.06/T^{1.1}$ tempts us to estimate the effective number of unquenched Ce^{3+} ions. If the Ce^{3+} ions were in the crystal-field ground state of $J_z = \pm 3/2$ in the hexagonal structure, then they would give rise to a Curie constant of 0.621 emu K/mol. The observed Curie constant of 0.06 emu K/mol corresponds to a concentration of 10% for such Ce^{3+} ions. On the other hand, the $M(B)$ curve in the inset changes from a linear dependence at 10 K to a nonlinear dependence at 0.5 K. The intercept of the linear extrapolation of the $M(B)$ curve at 0.5 K to $B=0$ gives a value of $0.05\mu_B/f.u.$, which is much smaller than the $0.13\mu_B/f.u.$ expected for the saturation moment for 10% Ce^{3+} ions in the $J_z = \pm 3/2$ state. Therefore, such an assumption of the presence of free Ce^{3+} ions is oversimplified, and it is conjectured that the magnetic moments induced from atomic disorder are partially quenched by the Kondo effect.

Figure 4 shows the temperature dependence of resistivity $\rho(T)$ for as-grown single crystals of CeRhSn and LaRhSn along the *a* and *c* axes. For LaRhSn, a sharp drop in $\rho(T)$ at 2 K is a superconducting transition that was reported previously.²² Two remarkable features for CeRhSn are the large maximum in $\rho_a(T)$ at 70 K and the high anisotropy, $\rho_a(T) = 2 - 5 \rho_c(T)$, over the whole temperature range. Both are more significant than those found in a valence-fluctuating system CeNiIn with the same type of crystal structure.²³ The large maximum in $\rho_a(T)$ can be attributed to the Kondo scattering of conduction electrons by $4f$ electronic states, in view of the very weak anisotropy for LaRhSn. In fact, the

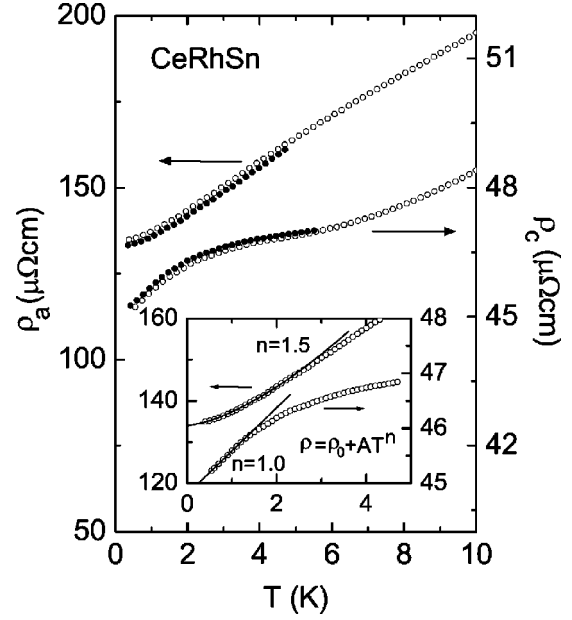


FIG. 5. Temperature dependence of the electrical resistivity ρ for single crystals of CeRhSn; as grown (open circles) and annealed at 900 °C for three weeks (filled circles). The inset shows the fits of the low-temperature data by $\rho(T) = \rho_0 + AT^n$.

magnetic contribution to the resistivity, $\rho_{ma} = \rho_a(\text{CeRhSn}) - \rho_a(\text{LaRhSn})$, is proportional to $-\ln T$ at high temperatures, as is shown in the inset of Fig. 4. The characteristic Kondo temperature T_K is the order of 100–200 K.

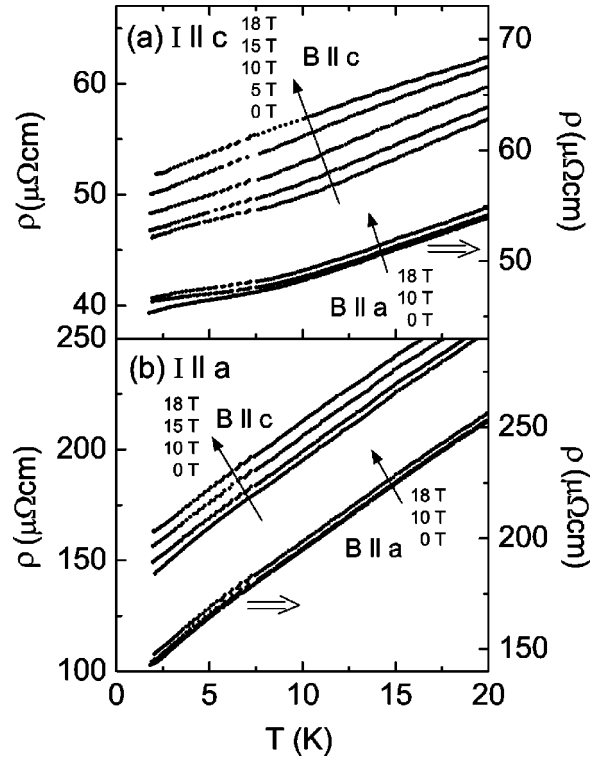


FIG. 6. Temperature dependence of the electrical resistivity ρ of the annealed single crystal of CeRhSn for (a) $I//c$ and (b) $I//a$ under various constant magnetic fields up to 18 T in longitudinal and transverse geometries.

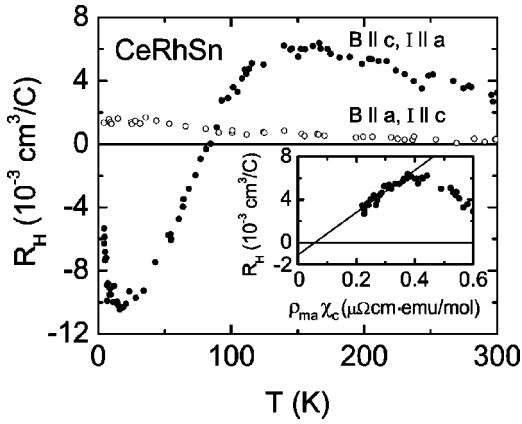


FIG. 7. Temperature dependence of the Hall coefficient R_H of the annealed single crystal of CeRhSn for $B//a$ ($I//c$) and $B//c$ ($I//a$). The inset shows a plot of R_H vs $\rho_m\chi$ where ρ_m is the magnetic contribution to the resistivity and χ is the magnetic susceptibility. The line represents a fit to the data of $R_H = R_0 + \alpha\rho_m\chi$ for $B//c$ ($I//a$) at $160 \text{ K} < T < 300 \text{ K}$.

It is interesting to note that the overall temperature dependence of $\rho_a(T)$ for CeRhSn is similar to that reported in Ref. 12 for a polycrystalline sample, while $\rho_c(T)$ is similar to that reported in Ref. 24. This may reflect the texture of polycrystalline samples prepared by arc melting. However, the fact that the values of residual resistivity, $\rho_a = 134 \mu\Omega \text{ cm}$ and $\rho_c = 44.8 \mu\Omega \text{ cm}$, are larger than those reported for polycrystalline samples^{12,24} cannot be explained by the effect of texture. We observed no decrease in the residual resistivity by annealing at 900°C for three weeks, as is presented in Fig. 5. In addition, the upward deviation in $\rho_c(T)$ for $T < 7 \text{ K}$ remains after the long-term anneal. The inset of Fig. 5 shows the fit of the low-temperature data with the equation $\rho(T) = \rho_0 + AT^n$. The values for n are 1.5 and 1.0 for ρ_a and ρ_c , respectively, which are larger than the $n = 0.75$ reported for a polycrystal.¹²

If the residual resistivity arises from coherent spin fluctuations, then application of sufficiently high magnetic field would suppress the spin fluctuations, and thus depress the resistivity significantly, as was observed in CePdAl.²⁵ Keeping this in mind, we measured the resistivity of CeRhSn in fields up to 18 T for both transverse and longitudinal configurations. The data of $\rho(T)$ in various constant fields are shown in Figs. 6(a) and 6(b) for $I//c$ and $I//a$, respectively. For all configurations, a positive shift is seen. We also measured the field dependence of resistivity at constant temperatures. At 2 K, the magnetoresistance as a function of $B//c$ is roughly proportional to B^2 for both $I//a$ and $I//c$. The effect for $B//c$ is much larger than that for $B//a$, which is understood by considering the high anisotropy of the magnetic susceptibility $\chi_c \gg \chi_a$. In zero field, $\rho_c(T)$ deviates upward from the linear behavior on cooling below 10 K. This deviation is suppressed upon increasing B above 15 T for $B//c$, while it remains for $B//a$. This field quench of the upward deviation suggests that there is an additional scattering mechanism originating from electronic spins with a characteristic temperature of 10 K.

Figure 7 shows the temperature dependence of the Hall

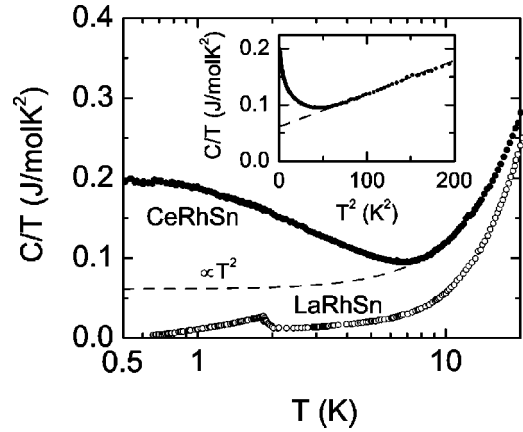


FIG. 8. Temperature dependence of the specific heat divided by temperature C/T plotted on a logarithmic T scale for the annealed single crystal of CeRhSn and the as-grown single crystal of LaRhSn. The C/T data for CeRhSn are replotted against T^2 in the inset. The broken lines are fits to the data of the formula $C/T = \gamma + \beta T^2$ for $8 \text{ K} < T < 15 \text{ K}$.

coefficient R_H for $B//a$ ($I//c$) and $B//c$ ($I//a$). In contrast to the monotonic increase of $R_H(B//a)$ with decreasing temperature, $R_H(B//c)$ exhibits a strong temperature variation with a positive maximum at 150 K and a negative minimum at 20 K. The high-temperature data above 160 K can be reproduced by the expression, $R_H = R_0 + \alpha\rho_m\chi$, where R_0 is the ordinary Hall constant and ρ_m is the magnetic contribution to the resistivity.²⁶ As is shown in the inset, the linear extrapolation of the $R_H(B//c)$ vs $\rho_m\chi$ plot to $\rho_m\chi = 0$ yields $R_0 = -1.0 \times 10^{-3} \text{ cm}^3/\text{C}$, which corresponds to a concentration of electron carriers of 0.37/f.u. For Ce-based Kondo or valence-fluctuating compounds, $R_H(T)$ at high temperatures is governed by skew scattering which gradually decreases as the coherence sets in.²⁷ This picture explains the gradual decrease in $R_H(B//c)$ for $T < 100 \text{ K}$. However, the sharp upturn below 20 K is unusual for a valence-fluctuating compound, but resembles the behavior reported for a disordered Kondo alloy $\text{CeCu}_{5-x}\text{Ga}_x$ at $T < 20 \text{ K}$, which was attributed to the anomalous velocity contribution.²⁸

Figure 8 shows the temperature dependence of the specific heat divided by temperature C/T for the annealed crystal of CeRhSn and the as-grown crystal of LaRhSn. With decreasing temperature, C/T for CeRhSn exhibits a minimum at 7 K, which is followed by the so-called non-Fermi-liquid behavior, $C/T \propto -\ln T$. Below 0.7 K, however, C/T is saturated to a rather large value of 0.2 J/mol K^2 . This saturated behavior is dissimilar to the divergent behavior in non-Fermi-liquid systems. It should be noted that the data have no anomaly at about 6.2 K, inconsistent with the previously reported one with a distinct jump, which remained after the anneal for eight days.¹² We confirmed that a polycrystalline sample annealed at 950°C for seven days showed no anomaly in the specific heat at 6.2 K either. In Fig. 8, the jump in C/T at 2 K for LaRhSn is associated with the superconducting transition. The magnetic entropy due to $4f$ electrons in CeRhSn was calculated by subtracting the data of C/T for LaRhSn from that of CeRhSn. With increasing temperature, the magnetic entropy passes through a plateau of

$0.3 R \ln 2$ at around 30 K, where R is the gas constant, and reaches $0.85 R \ln 2$ at 70 K, the highest temperature of our measurements. This magnitude of the magnetic entropy is consistent with the Kondo temperature of 100–200 K estimated from the $\ln T$ dependence of $\rho_m(T)$.

In the inset of Fig. 8, the C/T data are replotted against T^2 . Fitting to the data for $8 \text{ K} < T < 15 \text{ K}$ with the formula $C/T = \gamma + \beta T^2$ gives $\gamma = 0.061 \text{ J/mol K}^2$ and $\beta = 5.83 \times 10^{-4} \text{ J/mol K}^4$. The relation $\gamma = 0.18 \pi^2 R/T_K$ for a Kondo impurity with $J = 5/2$ (Ref. 29) yields the value of T_K to be 240 K. This T_K is considered as a characteristic temperature of the dominant portion of Ce ions in the valence-fluctuating state. On the other hand, the strong upturn in C/T on cooling below 7 K indicates the presence of low-energy excitations with a characteristic temperature of approximately 7 K. This temperature is close to the temperature at which the c -axis resistivity deviates upward from the linear dependence (see Fig. 6). It is recalled that at about 7 K the power for $\chi_c(T) \propto T^{-n}$ changes from $n = 0.45$ to $n = 1.1$ (see Fig. 3). The subtraction of the hypothetical T^2 dependence of C/T as drawn by the broken line from the observed data of C/T gives an estimation of the excess entropy to be 0.45 J/mol K , which is equal to $0.08 R \ln 2$. If this is attributed to Ce ions with a magnetic doublet ground state, then its concentration becomes 8% of the total Ce ions. This is in agreement with the fraction of 10% of Ce^{3+} ions estimated from the analysis of χ_c as was described above.

One possible origin for the non-Fermi-liquid-like behavior observed below 7 K is the atomic disorder, as was proposed by Ślebarski *et al.*¹² Although direct evidence of atomic disorder in CeRhSn has not yet been obtained, the presence of atomic disorder in an isostructural compound URhSn was suggested by the broad distribution of the hyperfine field at the Sn nucleus measured by ^{119}Sn Mössbauer spectroscopy.³⁰ Whereas the degree of such disorder in the Rh-Sn plane in CeRhSn might depend on the heat treatment, no effect of the annealing at 900°C for three weeks was observed in either the electrical resistivity or the magnetic susceptibility of single crystals. The present x-ray-diffraction analysis led to a very large value of the atomic displacement parameter only along the c axis for Rh atoms in the Rh-Sn plane, which may be related to the instability of the ZrNiAl-type structure. On the other hand, an anomalous increase in the c/a ratio on cooling below 120 K was found from neutron powder-diffraction experiments.¹² Further refinement of the crystal structure at low temperatures would be necessary to understand the anomalous physical properties of this compound.

IV. SUMMARY

We have reported a set of measurements of x-ray diffraction, magnetic susceptibility, electrical resistivity, magnetoresistance, Hall coefficient, and specific heat on single crystals of CeRhSn. The structural analysis suggested that the Ce $4f$ state is strongly hybridized with the $4d$ band derived from the Rh2 atoms, consistent with the previous band-structure calculation.¹² This out-of-plane hybridization in the hexagonal structure may be responsible for both the anisotropic resistivity and valence-fluctuating behavior with the characteristic temperature of 200 K. On cooling below 7 K, some sort of low-energy excitation manifests itself in the following behaviors. The resistivities along the a and c axes, respectively, deviate downward and upward from the extrapolation from high temperatures. The c -axis susceptibility exhibits a Curie-like behavior down to 0.4 K. Furthermore, the specific heat divided by temperature turns up below 7 K, and saturates to a rather large value of 0.2 J/mol K^2 at 0.5 K. Therefore, CeRhSn is a rare example of low-energy excitations manifesting themselves at low temperatures in the valence-fluctuating state. Such a phenomenon has been recently found in a Ce-filled skutterudite $\text{CeRu}_4\text{Sb}_{12}$,^{31,32} but its origin is not yet been understood. In all measurements of the single-crystal CeRhSn, no distinct anomaly was observed at about 6.2 K, in contrast to the previous report on a polycrystalline sample.^{12,21} The large value of the residual resistivity was not decreased by the annealing at 900°C for three weeks. On the other hand, application of magnetic fields up to 18 T yielded a positive magnetoresistance. These observations suggest that the low-temperature anomalies in CeRhSn originate not from coherent spin fluctuations but from some sort of disorder in this compound. In order to study the type of disorder and its role in the low-energy excitations, microscopic studies using NMR and muon-spin relaxation are in progress.

ACKNOWLEDGMENTS

The authors wish to thank Y. Shibata for the electron-probe microanalysis, S. Yamanaka for the generous use of the x-ray-diffraction analyzer, and A. Ślebarski and K. Łatka for valuable discussions. This work was supported by a grant for an International Joint Research Project from the NEDO, the COE Research (Grant No. 13CE2002) in a Grant-in-Aid from MEXT Japan, and the U. S. Department of Energy under Grant No. DE-FG03-86ER-45230.

*Present address: National Research Laboratory for Materials Science, Korea Basic Science Institute, Daejeon 305-333, South Korea.

¹T. Takabatake, F. Iga, T. Yoshino, Y. Echizen, K. Katoh, K. Kobayashi, M. Higa, N. Shimizu, Y. Bando, G. Nakamoto, H. Fuji, K. Izawa, T. Suzuki, T. Fujita, M. Sera, M. Hiroi, K. Maewaza, S. Mock, H. v. Löhneysen, A. Brückl, K. Neumaier, and K. Andres, *J. Magn. Magn. Mater.* **177–181**, 277 (1998).

²D. T. Adroja, S. K. Malik, B. D. Padalia, and R. Vijayaraghavan, *Phys. Rev. B* **39**, 4831 (1989).

³S. K. Malik and D. T. Adroja, *Phys. Rev. B* **43**, 6277 (1991).

⁴S. Yoshii, M. Kasaya, H. Takahashi, and N. Mori, *Physica B* **223&224**, 421 (1996).

⁵N. Harish Kumar and S. K. Malik, *Phys. Rev. B* **62**, 127 (2000).

⁶T. Sasakawa, T. Suemitsu, J. Kitagawa, O. Sologub, P. Salamakha, and T. Takabatake, *J. Phys.: Condens. Matter* **14**, L1

- (2002).
- ⁷Ch. D. Routsis, J. K. Yakinthos, and H. Gamari-Seale, *J. Magn. Mater.* **117**, 79 (1992).
- ⁸R. Ferro, R. Marazza, and G. Rambaldi, *Z. Metallkd.* **65**, 37 (1974).
- ⁹R. Ferro, R. Marazza, and G. Rambaldi, *Z. Anorg. Allg. Chem.* **410**, 219 (1974).
- ¹⁰V. I. Zaremba, Y. M. Kalychak, V. P. Dubenskiy, R.-D. Hoffmann, and R. Pöttgen, *J. Solid State Chem.* **152**, 560 (2000).
- ¹¹R. Mishra, R. Pöttgen, R.-D. Hoffmann, H. Trill, B. D. Mosel, H. Piotrowski, and M. F. Zumdick, *Z. Naturforsch.* **56b**, 589 (2001).
- ¹²It is interesting to note that the overall temperature dependence of $\rho_a(T)$ for CeRhSn is similar to that reported in Ref. 12 for a polycrystalline sample, while $\rho_c(T)$ is similar to that reported in Ref. 24. This may reflect the texture of polycryst., 589 (2001).
- ¹³A. Ślebarski, M. B. Maple, E. J. Freeman, C. Sirvent, M. Radłowska, A. Jezierski, E. Grando, Q. Huang, and J. W. Lynn, *Philos. Mag. B* **82**, 943 (2002).
- ¹⁴A. H. Castro Neto, G. Castilla, and B. A. Jones, *Phys. Rev. Lett.* **81**, 3531 (1998).
- ¹⁵D. Huo, T. Kuwai, T. Mizushima, Y. Isikawa, and J. Sakurai, *Physica B* **312–313**, 232 (2002).
- ¹⁶Y. Isikawa, T. Mizushima, N. Fukushima, T. Kuwai, J. Sakurai, and H. Kitazawa, *J. Phys. Soc. Jpn.* **65**, 117 (1996).
- ¹⁷A. Dönni, G. Ehlers, H. Maletta, P. Fischer, H. Kitazawa, and M. Zolliker, *J. Phys.: Condens. Matter* **8**, 11 213 (1996).
- ¹⁸M. S. Kim, Y. Echizen, K. Umeo, T. Tayama, T. Sakakibara, and T. Takabatake, *Physica B* **329–333**, 524 (2003).
- ¹⁹T. Sakakibara, H. Mitamura, T. Tayama, and H. Amitsuka, *Jpn. J. Appl. Phys., Part 1* **33**, 5067 (1994).
- ²⁰G. M. Sheldrick, computer code SHELXL-97, Program for Crystal Structure Refinement (University of Göttingen, Germany, 1997).
- ²¹R. Pöttgen, A. Lang, R.-D. Hoffmann, B. Künnen, G. Kotzyba, R. Müllmann, B. D. Mosel, and C. Rosenhahn, *Z. Kristallogr.* **214**, 143 (1999).
- ²²A. Ślebarski, M. Radłowska, T. Zawada, M. B. Maple, A. Jezierski, and A. Zygmunt, *Phys. Rev. B* **66**, 104434 (2002).
- ²³F. Canepa and S. Cirafici, *J. Alloys Compd.* **232**, 71 (1996).
- ²⁴H. Fujii, T. Inoue, Y. Andoh, T. Takabatake, K. Satoh, Y. Maeno, T. Fujita, J. Sakurai, and Y. Yamaguchi, *Phys. Rev. B* **39**, 6840 (1989).
- ²⁵Y. Bando, T. Suemitsu, K. Takagi, H. Tokushima, Y. Echizen, K. Katoh, K. Umeo, Y. Maeda, and T. Takabatake, *J. Alloys Compd.* **313**, 1 (2000).
- ²⁶T. Goto, S. Hane, K. Umeo, T. Takabatake, and Y. Isikawa, *J. Phys. Chem. Solids* **63**, 1159 (2002).
- ²⁷A. Hamzić and A. Fert, in *Selected Topics in Magnetism*, edited by L. C. Gupta and M. S. Multani (World Scientific, Singapore, 1993), p. 131.
- ²⁸A. Fert and P. M. Levy, *Phys. Rev. B* **36**, 1907 (1987).
- ²⁹A. Hamzić, A. Fert, and E. Bauer, *Physica B* **171**, 263 (1991).
- ³⁰A. C. Hewson, *The Kondo Problem to Heavy Fermions* (Cambridge University, Cambridge, England, 1993), p. 185.
- ³¹R. Kruk, R. Kmiec, K. Łatka, K. Tomala, R. Troć, and V. H. Tran, *Phys. Rev. B* **55**, 5851 (1997).
- ³²N. Takeda and M. Ishikawa, *Physica B* **259–261**, 92 (1999).
- ³³E. D. Bauer, A. Ślebarski, R. P. Dickey, E. J. Freeman, C. Sirvant, V. S. Zapf, N. R. Dilley, and M. B. Maple, *J. Phys.: Condens. Matter* **13**, 5183 (2001).